3D ELECTRIC FIELD CALCULATION WITH SURFACE CHARGE METHOD

S. Yamada

National Institute of Radiological Sciences
4-9-1 Anagawa, Chiba 260, Japan

Abstract

This paper describes an outline and some examples of three dimensional electric field calculations with a computer code developed at NIRS. In the code, a surface charge method is adopted because of it's simplicity in the mesh establishing procedure. The charge density in a triangular mesh is assumed to distribute with a linear function of the position.

The electric field distribution is calculated for a pair of drift tubes with the focusing fingers on the opposing surfaces. The field distribution in an acceleration gap is analyzed with a Fourier–Bessel series expansion method. The calculated results excellently reproduces the measured data with a magnetic model.

Introduction

An interdigital–H type linac[1] is very effective for heavy ion acceleration because of its excellently high shunt impedance. A size of the acceleration cavity is reasonable even for relatively low operation frequency of less than about 100 MHz. In order to make the better use of such characteristics of an IH linac, it is very much desired to reduce the capacitance between opposing drift tubes. An RFQ structure proposed by D. Boussard[2], which is sometimes called as a fingered drift tube linac (FDTL), may be one of the best solution for reducing the total capacitance without losing the transverse acceptance.

An analytic expression is given by D. Boussard for the electric field distribution in an acceleration gap of the FDTL, putting a crude assumption on the boundary conditions. To get precise values of the field distribution, however, the numerical three dimensional calculation is required, because the fingered drift tube (FDT) has not a cylindrical symmetry. A computer code POT3D is developed mainly for getting the acceleration and focusing efficiencies of the FDTL. The code is expected to be effective for the estimation of the capacitance between two FDT electrodes. This information is very important to predict a resonant frequency of the cavity and a gap voltage distribution along the beam axis. The computer code is also applicable to a 4–vane type RFQ electrodes to calculate the reduction factor of A_{10} coefficient originally pointed out by K. Crandall[3] at LANL.

Outline of the surface charge method

A surface charge method is adopted for the POT3D code, because this method requires the most simple procedure for establishing a mesh. Apart from a widely used two dimensional codes, the surface charge method requires meshes only on the surfaces of the electrodes. The charge density is assumed to be a linear function of the position in a triangular mesh on the conductor surface.

The potential at any point identified by a position vector $\vec{r}$ is given by the following equation

$$U(\vec{r}) = \sum_i \int_{S_i} \sigma(\vec{s}) G(\vec{r}, \vec{s}) \mathrm{d}\vec{s}, \tag{1}$$

where $\sigma(\vec{s})$ is a charge density induced on the conductor surface, and $G(\vec{r}, \vec{s})$ is the potential produced at the point $\vec{r}$ by a unit charge located at the position $\vec{s}$ on the ith conductor surface.

The charge density $\sigma(\vec{s})$ is assumed to be linear with the position $\vec{s}$. Then $U(\vec{r})$ is represented by a weighted summation of the charge densities at the mesh intersects. Since Eq.(1) is also valid for any point on the conductor surface, we get a set of such linear equations for all mesh points. In the surface charge method, the charge density distribution on the conductor surfaces is directly obtained by solving such set of the combined linear equations.

The electric field components are also described by an analytic equation similar to Eq.(1) and calculated more precisely than the conventional numeric codes using a difference equation or other methods which need the numerical differentiation. The field strength of this method, however, cannot give a correct value on the mesh boundary, since the charge density and its derivative are not continuous on the boundary lines.

Multipole expansion of the electric field

The electrostatic potential having a periodicity of L in z direction can be expanded into a Fourier–Bessel series of

$$U(r, \varphi, z) = \frac{V_g}{2} \sum_{m=0}^{\infty} \sum_{n=0}^{\infty} F_{nm}(r) \cdot \cos m\varphi \cdot \cos nkz, \tag{2}$$

where a cylindrical coordinate system (r, φ, z) is adopted. The symbol k stands for the wave number $k = 2\pi/L$ and the radial function $F_{nm}(r)$ is given by the following equations

$$F_{0m}(r) = A_{0m} \cdot r^m \tag{3}$$
$$F_{nm}(r) = A_{nm} \cdot I_m(nkr). \tag{4}$$

The multipole field amplitude, A_{nm}, is obtained by doubly integrating the potential function through a half period in z and φ directions:

$$A_{00} = \frac{2}{\pi^2 V_g} \int_0^{\pi} \int_0^{\pi} U(r, \varphi, z) \mathrm{d}\varphi \mathrm{d}\xi \tag{5}$$

$$A_{0m} = \frac{4}{\pi^2 r^m V_g} \int_0^{\pi} \int_0^{\pi} U(r, \varphi, z) \cos m\varphi \mathrm{d}\varphi \mathrm{d}\xi \tag{6}$$

$$A_{n0} = \frac{4}{\pi^2 I_0(nkr) V_g} \int_0^{\pi} \int_0^{\pi} U(r, \varphi, z) \cos n\xi \mathrm{d}\varphi \mathrm{d}\xi \tag{7}$$

$$A_{nm} = \frac{8}{\pi^2 I_m(nkr) V_g} \int_0^{\pi} \int_0^{\pi} U(r, \varphi, z) \cos m\varphi \cos n\xi \mathrm{d}\varphi \mathrm{d}\xi, \tag{8}$$

where V_g is a potential difference between two adjacent electrodes for a FDTL and will be replaced by an intervane voltage, V_v, for an RFQ electrode.

Using the A_{nm} coefficients given above, the electric field components are represented by

$$E_z = \frac{V_g}{2} \sum_{m=0}^{\infty} \sum_{n=1}^{\infty} nk A_{nm} I_m(nkr) \cdot \cos m\varphi \cdot \sin n\xi \tag{9}$$

$$E_r = -\frac{V_g}{2} \sum_{m=0}^{\infty} m A_{0m} r^{m-1} \cos m\varphi - \frac{V_g}{2} \sum_{m=0}^{\infty} \sum_{n=1}^{\infty} nk A_{nm} I'_m(nkr) \cos m\varphi \cos n\xi, \tag{10}$$

where $\xi = kz$.

With these equations, the electric field in a region of interest is expanded to a series of multipole components. A component, which mainly contributes to the beam acceleration, has $n = 1$ and $m = 0$, whereas the terms with A_{n2} act as the focusing forces.

A transit time factor for a drift tube linac is defined as an integration of E_z multiplied by $\sin \xi$ and is given by

$$T = \frac{\pi}{4} \sum_{m=0}^{\infty} A_{1m} I_m(kr) \cos m\varphi. \tag{11}$$

Usually, a value on the beam axis is adopted as a TTF. Even in a square wave approximation of the acceleration field, it is easy to show that the first term in Eq.(11) gives main contribution to the energy gain across the gap.

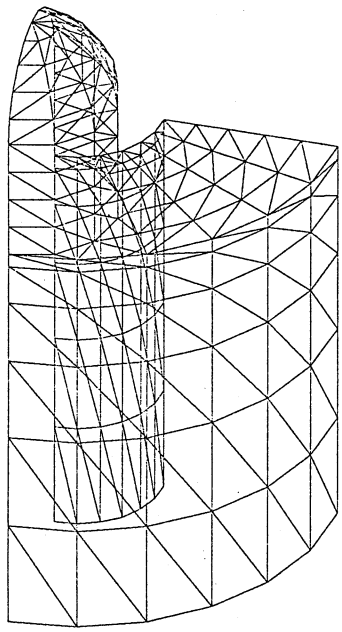

Fig. 1: An example of the generated mesh for a FDT electrode.

Only the first term of this series expansion exists in an acceleration field generated by a set of ideal 4-vane type RFQ electrodes, and the factor A_{10} is simply described as an acceleration efficiency A in a conventional RFQ beam dynamic theory. A transit time factor in the RFQ theory is defined to be $\pi/4$.

Brief description of the code

Similar to the SUPERFISH program, the computer code POT3D is divided into three program steps. The first step of the code, MESH3D, generates the triangular meshes on the conductor surfaces. A cylinder, a sphere, a sector *etc.* are defined as macro commands and can be used to simplify the mesh generating procedure. The commands to generate a FDT electrode and an RFQ vane are also prepared.

The second step, POT3D, establishes and solves the combined linear equations described above. For getting the solution of the combined equation, a Gauss-Jordan type sweep out method is applied. Throughout this step, the double precision calculations are adopted to minimize the computational errors.

The third step of the code, OUT3D, calculates the potential and field strength at any given position. The major part of this step is just the same as POT3D step except that a single precision calculation is used in this step. The mathematical data processing, the multipole coefficients calculation for an example, is done in the third step.

The numerical data which describes the meshes, the charge densities *etc.* are written as a file and read by the next steps. The overall codes are written with FORTRAN77 and run on a VAX-8250 computer (1.4 MIPS). A typical CPU time required by a FDT analysis is around 3000 sec.

Calculated results for FDT electrodes

Figure 1 shows an example of the generated mesh for a FDT electrode. Since the data input of some symmetry conditions are acceptable by the code, the mesh is generated only on 1/8 conductor surfaces for this case. The reduction in the number of mesh points is very effective to shorten the computational time. The focusing finger is assumed to have a cylindrical shape with a half sphere on the top.

The calculated field distributions are given in Fig. 2 with the open symbols. The solid curves in the figure, indicate the experimental results measured with a magnetic model[4]. Three different curves in (b) and (c) indicate the values at different axial positions. The normalization factor for the surface charge is calculated with E_z results and the same factor is used for E_y and E_x cases.

A transit time factor is calculated with the computer code, and gives very close value to that of a square wave approximation. The

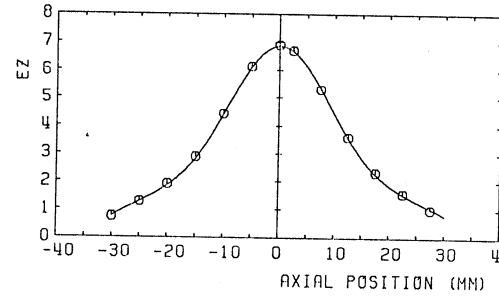

(a)

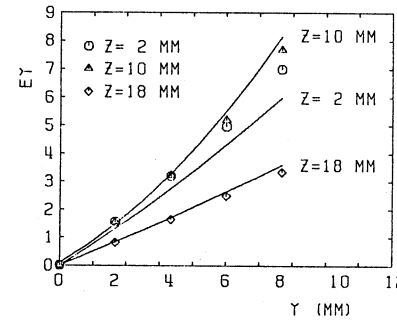

(b)

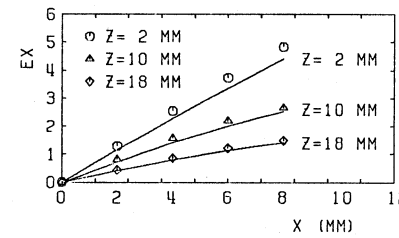

(c)

Fig. 2: (a) An example of the calculated acceleration field, E_z (open symbols). The solid curve indicates the experimental results measured with a magnetic model. The transverse field components (b) E_y and (c) E_x are also given as functions with the positions along y and x directions, respectively. Three different curves in (b) and (c) indicate the field strength at different axial positions. Normalization factor of the surface charge is the same for all figures.

contribution from the higher order terms is very small even for the off axis beams. These results make it very simple to describe the beam dynamics through a FDTL, because an energy gain at the gap is almost independent from radial positions. The analytic method of Boussard, however, gives completely different dependence on a gap to cell length ratio. This may come from too much simplification about the boundary conditions of the potential function in his expression.

The multipole analysis of the transverse electric field is also done for the same configuration of drift tubes. An example of the calculated results is shown in Fig. 3 together with the experimental curves measured by a small rotating coil with an FFT analyzer. The calculated values include up to $n = 4$ harmonics both for $m = 2$ and $m = 4$ results. The $m = 4$ component may be in a region of the experimental error, since odd m components are observed with nearly equal amplitudes. The overall agreement is very good both in longitudinal and transverse field components.

Discussions

The multipole components of A_{10} is calculated for 4-vane type RFQ electrodes. The reduction of this factor sometimes seriously affects on the acceleration characteristics of two dimensionally machined

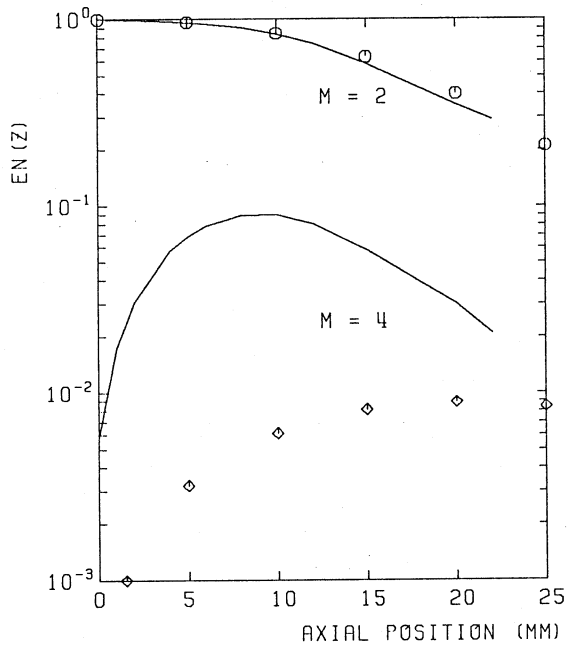

Fig. 3: The multipole field strength as functions with axial position. The solid curves indicate the experimental results measured with a small rotating coil. The calculated results are a summation of the field components up to $n = 4$. The $m = 4$ curve is in a region of the experimental error.

vane tops[3]. The calculated results very well reproduces the table given by K. Crandall both for the vanes with a constant radius and with variable radii. The difference between two calculations is about 1% or less. An example of a mesh used in a field calculation for RFQ electrodes is shown in Fig. 4.

It has been clear that POT3D gives excellent results for 3D electric field calculation. The beam dynamic design of FDTL will be easily done without time consuming model measurements, since the electric field distribution in the acceleration gap is fully predictable with this code. The capacitance between the opposing FDT electrodes will also give the very important knowledge to calculate the IH cavity geometry.

As a next target of this code, an effective length of an electric quadrupole electrode will be obtained with reasonable accuracy in near future. The interference effects of two adjacent electrodes will also be checked.

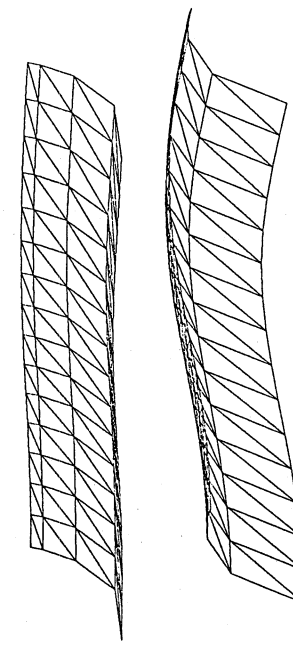

Fig. 4: An example of the generated mesh for RFQ electrodes.

Acknowledgments

Heartfelt thanks go to Prof. Hattori at Tokyo Institute of Technology who gave me the experimental results for FDT electrodes, and fruitful discussions. He also thanks Dr. Hirao and other members of the Division of Accelerator Physics at NIRS for their continuous encouragements and valuable discussions.

References

(1) for an example, Nolte, *et al*, Nucl. Instrum. & Methods, **201**, 281 (1982).

(2) D. Boussard, IEEE Trans. Nucl. Sci. **NS - 12, No. 3**, 648 (1965).

(3) K. Crandall, LANL Internal Rep., **LA - 9695 - MS** (1983).

(4) T. Hattori, *et al*, Proc. 6th Symp. on Accel. Sci. & Technol., 1987, Osaka, p101.